Available online at www.sciencedirect.com
SCIENCE DIRECT®
Energy and Buildings 37 (2005) 203–214
ENERGY and BUILDINGS
www.elsevier.com/locate/enbuild

An experimental study of energy consumption and thermal comfort for electric and hydronic reheats

Ji Gao, Ying Sun, Jin Wen[1], Theodore F. Smith*

Department of Mechanical and Industrial Engineering, The University of Iowa, Iowa City, Iowa 52242

Received 19 January 2004; received in revised form 2 March 2004; accepted 30 May 2004

Abstract

This paper compares the performances of electric and hydronic reheat modes for variable-air-volume units using experimental data for a building. The comparisons are made based on the daily energy consumption associated with each reheat mode and comfort performances within a building zone. Data are collected from a full-scale heating, ventilating, and air conditioning system. Weather conditions are considered and the corresponding energy distributions are evaluated. The results showed that the energy for the air handling unit using hydronic reheat is lower than that using electric reheat by about 24% when the air handling unit is operated in either the mechanical or mechanical and economizer cooling mode and 33% for the economizer cooling mode. The reheat energy for the variable-air-volume units using hydronic reheat is lower by about 75% than for electric reheat for either the mechanical or mechanical and economizer cooling mode and 54% for the economizer cooling mode. The main reason for the low-energy consumption using hydronic reheat is attributed to the lower requirement for the minimum air flow across the reheat coil. Electric reheat provides a slightly cooler comfort environment than that for hydronic reheat.

Keywords: Electric reheat; Hydronic reheat; Experimental data; Building energy

1. Introduction

Conversion from constant-air-volume systems to variable-air-volume (VAV) systems for heating, ventilating, and air-conditioning (HVAC) systems results in a significant reduction in building energy usage. The energy savings for VAV systems are a result of the reduced air flow. For example, a 75% reduction in fan energy requirements is realized by the reduced air flow [1]. Additional energy savings for VAV systems are realized in the cooling energy.

VAV systems provide multi-zone control with a single main duct. The supply air is maintained at a constant temperature, normally 12.8 °C, and the individual zone thermostats vary the air flow to the zone to maintain the desired zone temperature during the cooling season. Varying the zone air flow also reduces the cooling load on the cooling coil in an air handling unit (AHU) [2]. The reduction in cooling as the loads reduce occurs until the air flow reaches the minimum settings for indoor air quality requirements. If the damper for a VAV unit reaches the minimum position and the zone is still too cool, reheating of the air before it enters the zone is required to maintain comfort conditions in the zone. The reduced air flow that occurs when cooling loads are low or when heating is required results in reduced fan power.

A VAV with reheat system is common for HVAC systems [3] because it reduces electrical power by varying the supply fan speed and the air flow at part load [4]. An investigation [5] about the energy consumption and cost effectiveness of HVAC systems found that the VAV with reheat system is the most energy efficient system upgrade for older-type commercial office buildings that use a constant-air-volume system. The reheat is accomplished using either electric energy or hydronic energy. A study [6] based on building energy simulation showed that electric reheat consumes

* Corresponding author. Tel.: +1 319 335 5680; fax: +1 319 335 5669.
E-mail address: tfsmith@engineering.uiowa.edu (T.F. Smith).
[1] Present address: Department of Civil, Architectural and Environmental Engineering, Drexel University.

0378-7788/$ – see front matter
doi:10.1016/j.enbuild.2004.05.012

Nomenclature

Symbols

a, b	calibration coefficients
A	area (m^2)
c_1, c_2	curve-fit coefficients
CC	cooling coil energy (W h)
DD	degree-days (°C/day)
EE	electrical energy (W h)
ER	electric reheat energy (W h)
FE	fan energy (W h)
FW	fan power (W)
h_o	heat transfer coefficient (W/(m^2 K))
HE	natural gas energy (W h)
HR	hydronic reheat energy (W h)
I_{cl}	clothing thermal resistance
$K_{w,r}$	water reference property/unit factor (W/(L/s K))
M	metabolic heat production (W/m^2)
N	number of conditions
PE	pump energy (W h)
PMV	predicted mean vote
q	heat transfer (W)
Q	volumetric flow (L/s)
S	solar flux (W/m^2)
t	time (min)
t_{oe}, t_{os}	end and start occupied time (min)
t_{sr}, t_{ss}	sunrise and sunset times (min)
Δt	time interval (min)
T	temperature (°C)
TE	total energy (W h)
V	velocity (m/s)
W	mechanical work (W/m^2)
ϕ	relative humidity (%)

Subscripts

a	local air condition
cw	chilled water
cl	cooling
d	daily
dd	degree days
e	entering
ec	economizer
i	counter
ht	heating
l	leaving
oa	outdoor air
oc	occupied
om	overall mean
os, oe	people occupied start and end
r	room
rad	radiation
ref	reference
s	solar
set	reference point
sp	set point
ss, sr	sun rise, sun set
w	water
x, y, z	directions for a Cartesian coordinate system

Acronyms

AHU	air handling unit
HVAC	heating, ventilation, and air-conditioning
PI	proportional integral control algorithm
VAV	variable-air-volume

significantly more energy compared to that for hydronic reheat. The savings are greater during the summer months when the heating load is reduced. On average, the hydronic reheat energy is about 80% lower than that for electric reheat.

An investigation [7] indicates that electric reheat has more advantages, such as lower first costs and lower maintenance costs, than hydronic reheat for a VAV system. A state standard [7] mandates the use of hydronic reheat in VAV systems, making the assumption that the source energy usage for electric reheat is three times higher than that for hydronic reheat. However, it was found that this assumption neglects the energy losses associated with a hydronic system. Studies [7] suggested that a poorly controlled hydronic system might use as much or more energy as a well-controlled electric system. Energy savings will be consistent over the life of the equipment [8]. According to a study using campus buildings [9], electric reheat is more costly due to (1) the losses for generating and transmitting electricity and (2) that using natural gas directly to provide heated water for hydronic reheat is three times as efficient as electric reheat.

Besides energy consumption, indoor air quality has received considerable attention in the recent years. If HVAC systems are not able to control air contaminants and ensure thermal comfort within a zone, then complaints related to air quality occur. A common thermal comfort index is the predicted mean vote (PMV) [10]. To ensure a comfortable indoor climate, it is recommended maintaining PMV at 0 with a tolerance of ±0.5. Thermal comfort characterized by PMV is another factor to be considered when electric and hydronic reheats are compared.

In summary, studies that provide a comprehensive comparison of the energy consumption and thermal comfort for electric and hydronic reheat for an HVAC system are lacking. The related simulation results show that hydronic reheat consumes less energy compared to electric reheat. Another study suggests that electric reheat has an advantage compared to hydronic reheat when pumping energy and piping heat losses associated with hydronic reheat are considered. A comparison of the energy consumption and thermal comfort for electric and hydronic reheat based on experimental data is needed.

The objective of this study is to examine building energy consumptions by HVAC systems and comfort conditions using electric and hydronic reheats. Data uncertainty analyses for energy and PMV are reported for these comparisons to assist the discussion. Installation, operation, and maintenance costs for each reheat are other factors that could be considered in future research but are not the focus of this study.

Section 2 presents descriptions for the experimental equipment, setup, control sequences, and data for the tests. Section 3 explains the data reduction and uncertainty analysis. Section 4 gives results and discussions. Conclusions from this study are discussed in Section 5.

2. Experiment description

2.1. Test systems

Tests were conducted using the A- and B-Systems of the building facility of the Iowa Energy Center [11]. A schematic diagram of the floor plan for the facility is shown in Fig. 1. The facility is divided into three major areas, the general area and two sets of rooms, designated A- and B-Rooms, consisting of exterior rooms that face east, south, and west and are exposed to an exterior environment and interior rooms that are exposed only to interior conditions. AHU-A and AHU-B provide conditioned air for the A- and B-Rooms and are operated in the VAV mode. The AHUs and rooms are referred to as the A- and B-Systems. A schematic diagram for AHU-A and -B is shown in Fig. 2. Central heating and cooling plants serve both AHUs.

The temperature in a room is regulated with a VAV with reheat unit located in the plenum above a room. A schematic diagram of a VAV unit is shown in Fig. 3. The hydronic reheat is downstream of the electric reheat. A valve located in the return pipe controls the water flow through the hydronic reheat coil.

Sensors are available to measure air flows, temperatures, and humidities; entering, leaving, and mixed water temperatures as well as water flows for the AHU heating and cooling coils; and electrical power consumed by the pumps and fans. The air flow for a room is evaluated using a differential pressure sensor attached to a flow ring located near the entrance of the VAV unit and is regulated by varying a damper position. Sensors to measure entering and discharge air temperatures, volumetric water flow, as well as entering and leaving water temperatures for a hydronic reheat coil as well as power dissipated by an electric reheat coil are available. For the purpose of evaluating comfort, each room is equipped with comfort sensors that measure local air temperature, humidity, and speed and are located on a stand that is placed near the center of a room. Sensors are available to measure the outdoor air temperature, humidity, and wind speed and direction, as well as global horizontal and beam solar energy fluxes.

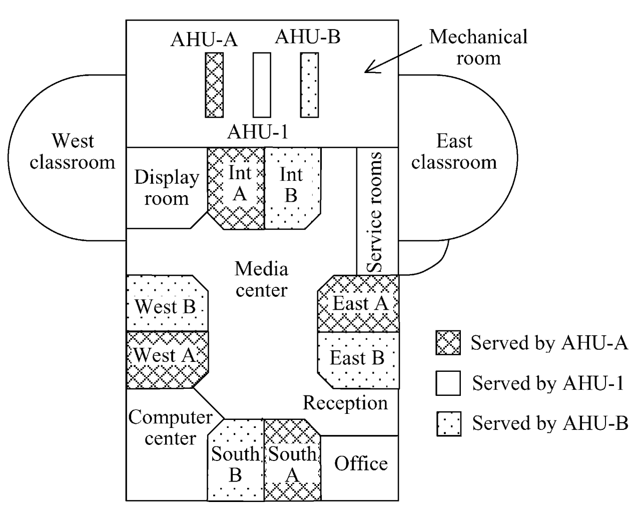

Fig. 1. Building facility [11].

2.2. Control sequences

The A- and B-Systems are controlled by direct digital controllers that are part of a commercial energy management and control system. The system operation, AHU controls for the supply air temperature, and the room controls for the VAV units are discussed in Sections 2.2.1–2.2.3 and are similar to those in a commercial building.

2.2.1. System operation

The system operation consists of four modes, that is, occupied mode, unoccupied mode with system off, night set-back mode, and system start-up mode. Because only the occupied and set-back modes are used in the tests, the unoccupied and start-up modes are not introduced. For the occupied mode, the fans, dampers, and valves are controlled with the normal control sequences using proportional integral control algorithms (PIs).

During the set-back mode, the room temperature, T_r, is compared with the corresponding heating and cooling room set-back mode setpoints, T_{sp-ht} and T_{sp-cl}. The system is in the dead-band when T_r in all rooms is between the corresponding T_{sp-ht} and T_{sp-cl}. Therefore, the fans are off, and the dampers and valves are closed. The set-back mode requires heating if T_r in a room drops below the corresponding T_{sp-ht} at which time the fans are turned on, and the AHU dampers and valves are 100% closed to re-circulate the building air. The electric or hydronic reheat is allowed to heat the air entering a room. The AHU stays in this state until T_r in all rooms rises above the corresponding T_{sp-ht} plus an adjustable differential (normally 0.6 °C). The set-back mode requires cooling if T_r in a room rises above the corresponding T_{sp-cl} at which time the fans are turned on, and the dampers and valves are controlled with the normal control sequences to drive supply air temperature, T_{sa}, to a supply air setpoint, T_{sp-sa}. The damper in each VAV unit is regulated to supply sufficient cool air to the room. The AHU stays in this state until T_r in all rooms drop below the corresponding T_{sp-cl} minus an adjustable differential (normally 0.6 °C).

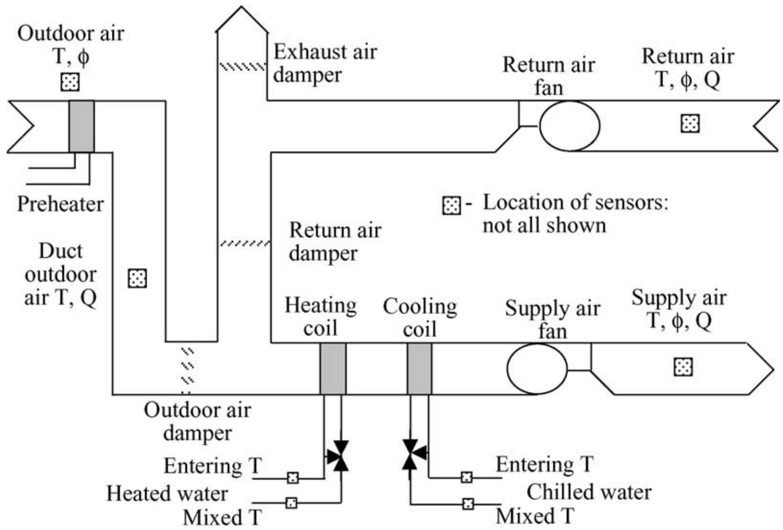

Fig. 2. Air-handling unit [11].

2.2.2. Supply air temperature control sequence

The control sequence used to maintain T_{sa} is divided into four control modes, namely, mechanical cooling, mechanical and economizer cooling, economizer cooling, and mechanical heating, as shown in Fig. 4. The modes correspond to the output from a single PI that is split to control the heated water coil valve, the AHU dampers, and the cooling coil valve.

Mechanical cooling or mechanical and economizer cooling exist when the cooling coil is needed to maintain the supply air temperature, that is, the output from the PI corresponds to a valve position from 0 to 100% open. For mechanical cooling, the outdoor air damper is held at the minimum position because either the outdoor air temperature, T_{oa}, or humidity, ϕ_{oa}, are above the temperature or humidity economizer setpoint, T_{sp-ec} or ϕ_{sp-ec}. For mechanical and economizer cooling, the damper is fully open because T_{oa} and ϕ_{oa} are less than T_{sp-ec} and ϕ_{sp-ec}.

As T_{oa} drops, the control sequence switches to the economizer cooling mode, where T_{sa} is maintained by modulating the outdoor air damper to mix outdoor air with re-circulated air. The control sequence for maintaining T_{sa} has a lower priority than maintaining a ventilation constraint that requires a minimum outdoor air flow. The minimum outdoor air flow is maintained by a minimum damper position. Because one PI loop is used to control different devices, there exists a period when the minimum damper position (typically 30% open) is reached but the PI loop output is not operating the heated water valve. During this period, there is no control for T_{sa} and T_{sa} may deviate from its set point.

If T_{oa} continues to decrease, a point is reached where the outdoor air damper is at the minimum position and mechanical heating is required. During the mechanical heating mode, the heated water coil valve is modulated by the PI to maintain T_{sa}.

2.2.3. VAV control sequences

The control sequence used to maintain T_r above T_{sp-ht} and below T_{sp-cl} is divided into VAV-heating and -cooling modes shown in Fig. 5. A dual PI is used to control T_r. During the cooling mode when T_r is above T_{sp-cl}, the VAV damper is modulated to bring in sufficient supply air and cool the room. This control sequence assumes that T_{sa} is lower than T_r. When T_r drops below T_{sp-ht}, a point is reached where the dual-PI output enters the heating mode. During the heating

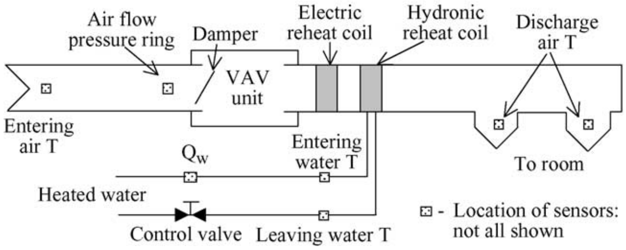

Fig. 3. VAV with reheat unit and associated equipment [11].

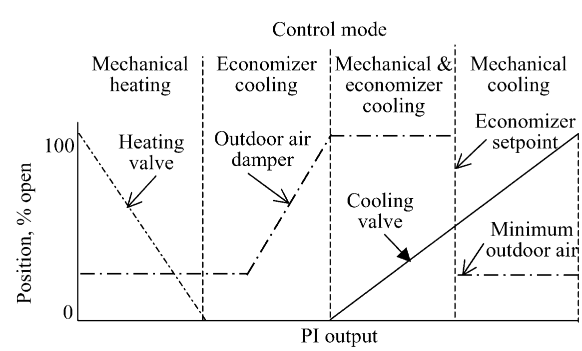

Fig. 4. Supply air temperature control sequence [11].

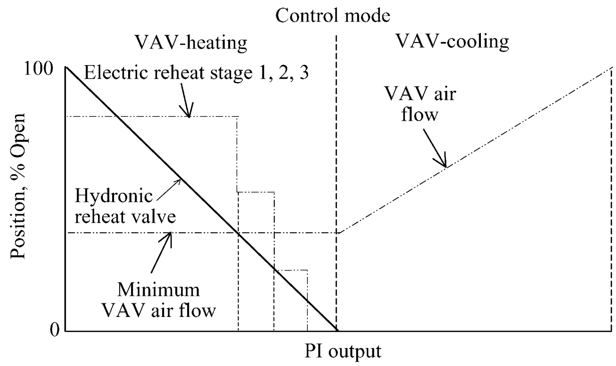

Fig. 5. Room temperature control sequence.

mode and if hydronic reheat is used, the reheat valve is modulated to keep T_r near $T_{sp\text{–}ht}$. If electric reheat is used, the hydronic reheat valve is closed and the stages of electric reheat are turned on in sequence as determined by the output of the dual PI. The stages of electric reheat are turned off in the same manner as they are turned on.

2.3. Test data

2.3.1. Test schedule

An analysis of energy usage for electric and hydronic reheat is based on the data from four tests, called Tests 1–4. Each test was conducted with a pattern shown in Table 1. The pattern shown in Table 1 is further divided into test periods of 1–4, with a total of 12 days per test. Two sequential days are set for periods 1 and 4, where the A- and B-Systems have the same reheat modes. Four sequential test days are set for periods 2 and 3, where the A- and B-Systems have different reheat modes. The alternating of electric (E) and hydronic (H) reheat between the A- and B-Systems is to account for any differences that may exist between the systems and any weather changes. For each test day, either E or H reheat is applied to the A- and B-Systems (A and B). There are four test patterns based on the reheat mode, namely, H(A)H(B), H(A)E(B), E(A)H(B), and E(A)E(B). To avoid the impact of unsteady state conditions from the previous day, data for the succeeding days except the first day in each period are selected for the analysis. Because there are only minor interactions between the A- and B-Systems, tests are interpreted as being applied to two independent HVAC systems and buildings.

Due to bad data and test settings, the patterns for Tests 2 and 3 deviated from that in Table 1. The pattern for Test 2 was H(A)H(B), E(A)H(B), E(A)E(B), and H(A)E(B) and that for Test 3 is H(A)H(B), E(A)E(B), E(A)H(B), and H(A)E(B) for periods 1, 2, 3, and 4, with 2, 2, 3, and 3 test days.

The test days and bad data are summarized in Table 2. Also, the supply air temperature control modes, which reflect the weather conditions, are shown in the last column

Table 1
Typical test pattern[a]

System	Period 1		Period 2				Period 3				Period 3	
	1.1	**1.2**	2.1	**2.2**	**2.3**	**2.4**	3.1	**3.2**	**3.3**	**3.4**	4.1	**4.2**
A	H	**H**	H	**H**	**H**	**H**	E	**E**	**E**	**E**	E	**E**
B	H	**H**	E	**E**	**E**	**E**	H	**H**	**H**	**H**	E	**E**

[a]E and H, electric and hydronic reheats; bold letters denote selected day for data analysis.

of Table 2. The heating coils were not operated during the tests and are unlikely to operate under most winter conditions in Iowa. Therefore, the tests account for typical weather conditions year around.

2.3.2. Test conditions

The conditions for the tests represent those for a commercial office building. The AHUs for the A- and B-Systems were operated identically and both systems were operated with either electric or hydronic reheat to maintain T_r. Two control modes for system operation are selected, namely, occupied mode from 6:00 to 18:00 and set-back mode from 18:00 to 6:00. The rooms are assumed to be occupied for 10 h from 7:00 to 18:00 excluding the lunch time from 12:00 to 13:00 by two people each having a computer and desk lamp. Each person requires 9.4 L/s of outdoor air. To maintain air quality, the minimum flow for outdoor air is 75.5 L/s (4 rooms $\times$ 18.8 L/s = 75.2 L/s). For each room, two supply-air diffusers and plenum returns are used. For occupied times, the air flow ranges, for hydronic and electric reheat for an exterior room, are 94.4–472 and 212–472 L/s, and those for an interior room are 94.4–189 and 118–189 L/s. A higher minimum air flow for electric reheat is used to prevent damage to the coil wires. The air flow is off during set-back times. $T_{sp\text{–}ht}$ and $T_{sp\text{–}cl}$ are set at 21.1 and 22.2 °C for the occupied time and 15.6 and 26.7 °C for the set-back time. The window blinds are opened and the door of a room is closed.

$T_{sp\text{–}ec}$ or $\phi_{sp\text{–}ec}$ are 18.3 °C and 110% RH, and $T_{sp\text{–}sa}$ = 12.8 °C. The speed of the supply fan is modulated to maintain duct static pressure at a set point of 35.6 mm W.G. The speed of the return fan is maintained at 50% of the supply fan speed to assure that the rooms are pressurized.

There are a total of five time periods for a day, namely, setback, preconditioning, people-occupied, lunch, and

Table 2
Test days and cooling control modes

Test	Test days (total days)	Cooling mode
1	1 July 2000–12 July 2000 (12)	Mechanical
2	2 March 2001–17 March 2001 (16[a])	Economizer
3	12 June 2001–21 June 2001 (10[b])	Mechanical
4	11 September 2001–23 September 2001 (12[c])	Mechanical and economizer

[a] Except 4 March 2001–7 March 2001 (bad data).
[b] Except 21 June 2001 (bad data).
[c] Except 19 September 2001 (bad data).

cleaning. The time period of 6:00–7:00 is for preconditioning (either precooling or preheating) to make a room comfortable before it is occupied. A room is people-occupied from 7:00 to 18:00. The lunch and cleaning times are 12:00–13:00 and 21:00–22:00. The baseboard heater in a room is operated for the people-occupied and room cleaning times to simulate interior thermal loads and is on (1.0 kW) from 7:00 to 12:00, 13:00 to 18:00, and 21:00 to 22:00. The lighting stages 1 (195 W) and 2 (390 W) for each room are on for the people-occupied time and only stage 2 is on for the lunch and cleaning times.

The heated and chilled water pumps for AHU-A and -B are fixed speed pumps whereas those for the heated water loops with the hydronic reheat coils are variable speed. The thermal storage tank is used to dampen temperature fluctuations caused by chiller cycling. The boiler outlet water temperature set point is 60.0 °C.

3. Data reduction and uncertainty analysis

3.1. Energy calculation

As shown in Fig. 6, fuels used to operate the A- and B-Systems are electricity and natural gas. Because the electricity and natural gas consumptions for each system are not measured directly and the heating and cooling plants serve both systems, the energy usage by the various HVAC components must be determined either directly by measuring the electrical energy for a component or indirectly by using thermal energy balances for a component. The daily electric energy, EE, includes energy for the supply and return fans, FE; the pumps for the heating coil, cooling coil, and heated water loop, PE; and the electric reheat, ER. Because chilled water is produced using an electric-motor driven compressor, the energy consumed in the cooling coil, CC, is assigned to the electrical energy category. The daily natural gas energy, HE, is used to supply heated water for the heating coil, HC, and the hydronic reheat, HR. The total energy, TE, represents the sum of EE and HE. It should be recognized that TE is not used when the costs of energy to operate the building are accounted for because the energy costs for electricity and natural gas differ considerably.

To compare the two reheat modes, daily energy usages are calculated by summing up the instantaneous values for 24 h. For example, FE is given by

$$\mathrm{FE} = \frac{1}{60}\sum_{i=1}^{1440} \mathrm{FW}_i\,\Delta t \qquad (1)$$

where FWi is the instantaneous fan power, Δt is the time interval between readings (=1 min), and 60 is a time conversion factor.

The instantaneous water heat transfer for a hydronic reheat coil, $q_{w,i}$, is

$$q_{w,i} = K_{w,r}[c_1 + c_2(T_{w,e} - T_{ref})](a + bQ_{w,s}) \times (T_{w,e} - T_{w,l}) \qquad (2)$$

where $K_{w,r}$ = 4179 W(L/s K) − K is the reference property/unit factor for water at the reference temperature of T_{ref} = 20.0 °C and the curve-fit coefficients are c_1 = 1 and c_2 = −0.00054 1/°C. a and b are calibration coefficients for the water volumetric flow sensor for a room. As an example, the calibration coefficients for a particular room are a = −0.00076 L/s and b = 0.981. $Q_{w,s}$ is the water volumetric flow. $T_{w,e}$ and $T_{w,l}$ are the entering and leaving water temperatures. The three measured variables for the water heat transfer are $Q_{w,s}$, $T_{w,e}$, and $T_{w,l}$. HR for hydronic reheat is determined from Eq. (1) with FE replaced by HR and FW_i by $q_{w,i}$.

The chilled water heat transfer for a cooling coil, $q_{cw,i}$, is computed using

$$q_{cw,i} = K_{w,r}[c_1 + c_2(T_{cw,e} - T_r)]Q_{cw}(T_{cw,e} - T_{cw,m}) \qquad (3)$$

where Q_{cw}, $T_{cw,e}$, and $T_{cw,m}$ are the volumetric flow as well as entering and mixed water temperatures for the cooling coil.

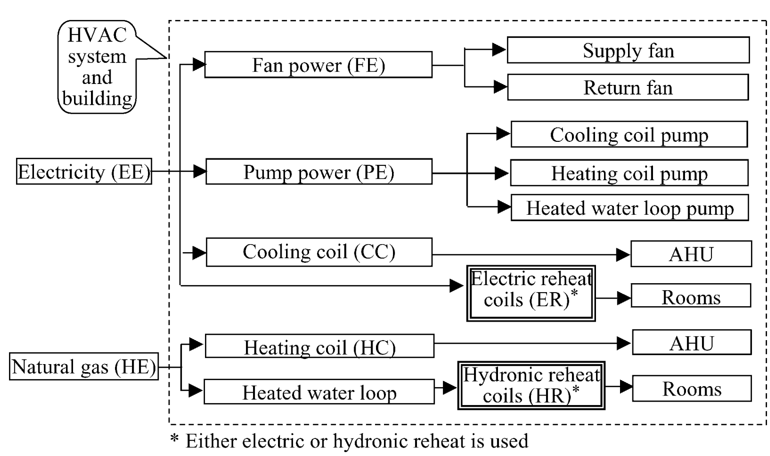

Fig. 6. Schematic diagram of electricity and natural gas energy usage.

CC is calculated using Eq. (1) by replacing FW_i with $q_{\mathrm{cw},i}$ and FE with CC.

3.2. Degree-days

It is expected that the energy consumed by the HVAC systems can be correlated with parameters that describe the state of the outside conditions. Weather related parameter that accounts for the consumed energy varying with the difference between an outdoor temperature and an interior temperature is daily degree-days, DD, [10] and is evaluated from:

$$\mathrm{DD} = \frac{1}{1440}\sum_{i=1}^{1440}(T_{\mathrm{oa}} - T_{\mathrm{set}})_i\,\Delta t \tag{4}$$

where T_{set} = 18.3 °C, which is the same as $T_{\mathrm{sp\text{–}ec}}$. Because the outdoor air temperature sensor was out of calibration for Tests 2 and 3, T_{oa} is approximated by a corrected outdoor air temperature.

The effect of solar energy is accounted in the solar-air temperature, $T_{\mathrm{oa\text{–}dd}}$, computed from

$$T_{\mathrm{oa-dd}} = T_{\mathrm{oa}} + \frac{S_{\mathrm{d}}}{h_{\mathrm{o}}} \tag{5}$$

where h_{o} is the heat transfer coefficient between the exterior building surface and the environment and is set to 28.4 W/(m^2 K) to represent 21.1 °C ambient still air [10]. S_{d} is the daily-averaged global horizontal solar flux is computed from

$$S_{\mathrm{d}} = \frac{1}{\Delta t_{\mathrm{s}}}\sum_{i=t_{\mathrm{sr}}}^{t_{\mathrm{ss}}} S_i\,\Delta t \tag{6}$$

where S_i is the instantaneous global horizontal solar flux that is recorded every minute by horizontal sensors that measures the combined beam and diffuse solar energy. The time interval to calculate S_{d} is given by $\Delta t_{\mathrm{d}} = t_{\mathrm{ss}} - t_{\mathrm{sr}}$, where t_{sr} and t_{ss} are the sunrise and sunset times [12] calculated for each day. Daylight savings time is accounted for when calculating the sunrise and the sunset times for Tests 1, 3, and 4 and is not included for Test 2 when standard time exists. Using $T_{\mathrm{oa\text{–}dd}}$, the solar degree-days, $\mathrm{DD_s}$, are calculated using

$$\mathrm{DD_s} = \mathrm{DD} + \frac{S_{\mathrm{d}}}{h_{\mathrm{o}}} \tag{7}$$

The values of $\mathrm{DD_s}$ are used for the discussions. In summary, the thermal load for a building is due in part to the temperature difference between the interior and exterior environments as well as the amount of solar energy irradiating the building. The degree-days account for the former load whereas the solar degree-days are an attempt to account for both loads.

3.3. Thermal comfort evaluation

Thermal comfort is evaluated using PMV [10]. The thermal sensation scale of +3, +2, +1, 0, −1, −2, and −3 represents hot, warm, slightly warm, neutral, slightly cool, cool, and cold feelings for people. PMV is a function of metabolic heat production, M; external work done by muscles, W; clothing thermal resistance, I_{cl}; room-air temperature, T_{a}; room mean-radiant temperature, T_{rad}; room air velocity near the person, V; and room relative humidity, ϕ. Because T_{rad} is not measured, it is taken as T_{a}. V is determined from $V = (V_x + V_y + V_z)/3$, where $V_i = Q/A_i$, $i = x, y, z$. Q is the room air flow. A_i is the floor or wall area for a room in the ith direction.

The comfort analysis is based on averaged values of PMV for the people-occupied time, $\mathrm{PMV_{oc}}$, calculated using

$$\mathrm{PMV_{oc}} = \frac{1}{\Delta t_{\mathrm{o}}}\sum_{i=t_{\mathrm{os}}}^{t_{\mathrm{oe}}} \mathrm{PMV}_i\,\Delta t \tag{8}$$

where PMV_i are the instantaneous values. The time interval for the occupied-averaged value is given by $\Delta t_{\mathrm{o}} = t_{\mathrm{oe}} - t_{\mathrm{os}}$, where t_{os} and t_{oe} denote the end and start of the people-occupied times. The overall mean values, $\mathrm{PMV_{om}}$, of $\mathrm{PMV_{oc}}$ for the four test patterns are obtained from

$$\mathrm{PMV_{om}} = \frac{1}{N}\sum_{i=1}^{N} \mathrm{PMV}_{\mathrm{oc},i} \tag{9}$$

N is the number of test days with the identical test pattern in each test. N is 3 for E(A) and H(B), 2 for H(A) and E(B) for Test 3. N is 4 for the other tests.

3.4. Uncertainty analysis

The overall uncertainty in a measurement [13] is a combination of the precision and bias limits. The uncertainty for an electric power measurement is about 0.3%. The relative uncertainty for the water volumetric flow measurements is about 0.6%. The uncertainty for the temperature measurements is ±0.14 °C. Using the propagation of the error [13] through the data reduction equations in Eqs. (2) and (3) and a correlation term because the temperature sensors are calibrated using the same temperature bath, the relative uncertainties for the hourly-average heat transfer are about 0.6%.

For PMV, the values for M, W, and I_{cl} are fixed and, therefore, their uncertainties are zero. The values for T_{a}, Q, and ϕ are data. The uncertainty analysis for PMV is based on four parameters, namely, T_{a}, T_{rad}, Q, and ϕ. Assuming that the parameters are independent of each other so that there are no correlation terms, the uncertainty for PMV is computed using the propagation of error analysis [13]. The uncertainties for T_{a}, Q, and ϕ are 0.14 °C, 1.2% of reading, and 2.1% of reading. These give a relative uncertainty for PMV of about 10.5%. The high uncertainty for PMV is because the temperature error terms are not reduced by a correlated term.

4. Results and discussions

4.1. Introduction

Excluding the days with bad data and settings, the four tests give a total of 27 days of data with each system being operated for at least 13 days on either electric or hydronic reheat mode. Because of the large amount of data, the discussion focuses on daily values. An important aspect of the analysis is to determine how the rooms respond on an instantaneous basis for electric and hydronic reheats. These results are presented in Section 4.2. Next, the comfort conditions for a room are examined in Section 4.3. Section 4.4 gives results for the major energy terms for the HVAC systems. The energy distributions for the systems as a function of the weather conditions and a comparison of electric and hydronic reheats are discussed in Section 4.5.

4.2. Instantaneous data

Data for the West B-Room for two days from Test 1, namely, 12 July 2000 for electric reheat and 02 July 2000 for hydronic reheat, are chosen to represent typical trends for the mechanical cooling mode. Similarly, data for the West B-Room for two days from Test 2, namely, 13 March 2001 for electric reheat and 03 March 2001 for hydronic reheat, are chosen for the economizer cooling mode. Data for VAV discharge-air, comfort, and room temperatures, electric reheat power, as well as hydronic reheat water flow are depicted in Figs. 7 and 8 for the mechanical and economizer cooling modes. The preconditioning and people-occupied time period of 6:00 (t = 360 min)–18:00 (t = 1080 min) is selected to present the data.

Electric reheat is active in Fig. 7a indicating that the entering air needs to be heated but hydronic reheat is off in Fig. 7b implying that the room does not need heating, where

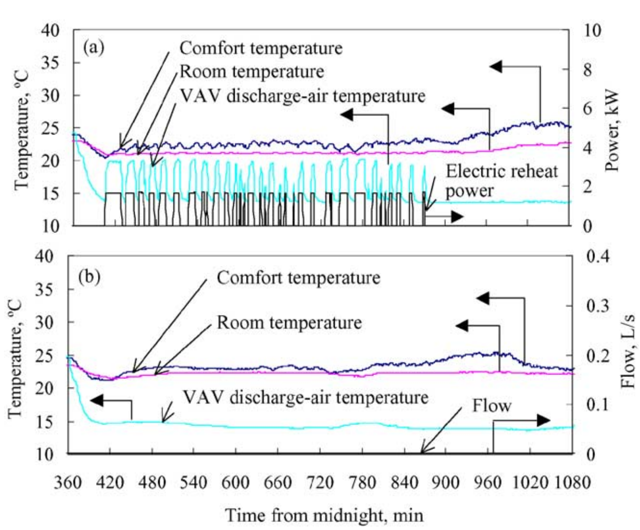

Fig. 7. Mechanical cooling mode for West B-Room. (a) Power and temperatures for electric reheat (12 July 2000); (b) Water flow and temperatures for hydronic reheat (2 July 2000).

the different operating conditions are caused by the higher minimum air flow for electric reheat because the weather conditions are similar for both days. The VAV damper is modulated in Fig. 7b to maintain room temperature. It is observed that the room temperatures are about 1.1 °C lower than the comfort temperatures for both the heating and cooling modes. Also, the curves of room temperatures are much smoother than those for the comfort temperatures, that is, the variation of room temperatures is much less intense than that of the comfort temperatures due to the locations of sensors for these temperatures.

From Fig. 7a, the electric reheat power is off at the beginning and the room temperature is cooled down below $T_{sp–ht}$. The reheat power starts with one-stage on (1.67 kW) at around 6:40 (t = 400 min) and then switches between one-stage on and off according to the variation of the room temperatures. In Fig. 7a, the comfort temperatures vary with the step change of the reheat power by about 1.1 °C for each power-on impulse and decrease slowly during the power-off period. The room temperatures require about 1 h, after the room is occupied (t = 420 min), for electric reheat and 2.5 h for hydronic reheat (Fig. 7b) to reach the room temperature setpoint. These results illustrate that the room temperatures respond about 1.5 h slower for hydronic than electric reheat; again this may be caused by the lower air flow for hydronic reheat.

From Fig. 8a, the electric reheat starts with three-stages on (5.00 kW) at the preconditioning and people-occupied time (t = 360 min) and switches to two-stages on when the room temperature is heated to $T_{sp–ht}$. Thereafter, the electric reheat switches between two-stages on (3.33 kW) and one-stage on (1.67 kW) according to the variation of the room temperature. Note that during the preconditioning and people-occupied time, the electric reheat is never off completely and is only off after t = 1080 min. The comfort temperatures vary with the variation of the electric reheat and increase about 1.1 °C for each impulse from one-stage on to two-stages and decrease slowly during the one-stage on periods.

From Fig. 8b, an impulse of the heated water flow of about 0.06 L/s causes 1.1 °C increase of the comfort temperature. Comparing Fig. 8a and b, it is observed that the room temperature takes about 0.5 h after the room is occupied for electric reheat and about 3.5 h for hydronic reheat to reach $T_{sp–ht}$. Therefore, the room temperatures respond about 3 h slower for hydronic reheat than for electric reheat.

From Fig. 8b, the room temperature does not reach 21.1 °C until around 10:40 (t = 640 min). That is, the occupants in the WB-room may feel uncomfortable at least 2 h after they enter the room at 7:00 (t = 420 min). During this time, the reheat water flow is at its maximum. One possible cause of this behavior is due to insufficient room air flow, which is held at its minimum. From Figs. 7b and 8b, the room temperatures reach peaks near 16:00 (t = 960 min) due to the heating by the solar energy in the afternoon and the room temperatures are out of control.

A factor that may affect the variation of the room temperatures is the placement of the hydronic reheat coil

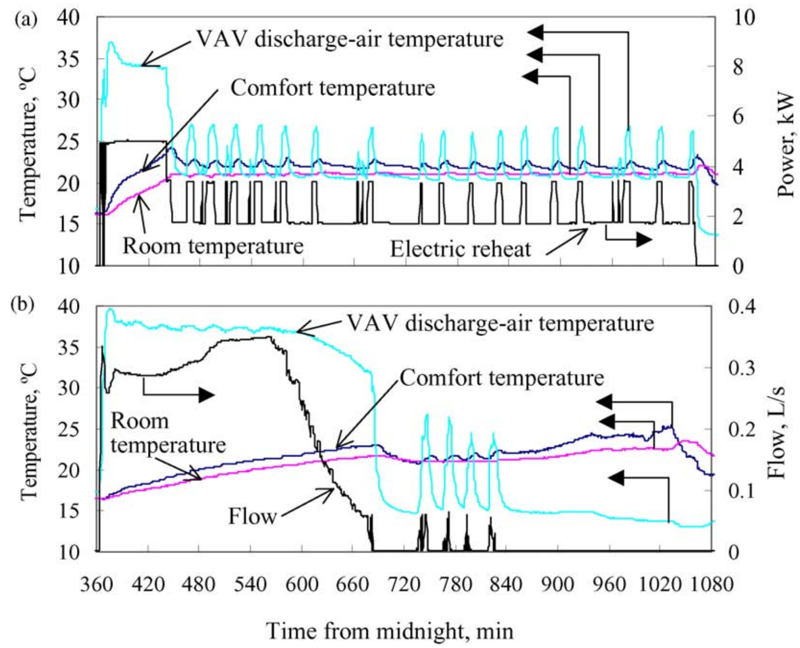

Fig. 8. Economizer cooling mode for West B-Room. (a) Power and temperatures for electronic reheat (13 March 2001); (b) Water flow and temperatures for hydronic reheat (3 March 2001).

downstream of the electric reheat coil. To examine this effect, the VAV discharge air temperatures are compared with the variation of electric reheat power. As observed from Fig. 7a, the VAV discharge-air temperatures increase by about 6.4 °C for each power-on stage. This result matches the temperature difference calculated using the air flow and one stage of electric reheat. The supply air temperature leaving the AHU is around 12.2 °C for this day, which means that the air temperature leaving the electric reheat is around 18.9 °C when the coil is on. Compared to the VAV discharge-air temperature in Fig. 7a, the air temperature leaving the hydronic reheat coil is around 19.4 °C, which is similar to the temperature leaving the electric reheat. Also, from Fig. 7a, there is almost no time delay between the VAV discharge air temperature and the variations of the electric reheat power. Similar observations are obtained from Fig. 8a. These results imply that the effect of hydronic reheat on air conditions, when the electric reheat operates, is small.

In summary, the instantaneous data show that the comfort temperatures fluctuate about 1.1 °C with a power stage on and off for electric reheat and vary smoothly with the variation of the water flow for hydronic reheat. The room temperatures respond about 1.5 h slower for Test 1 and 3 h slower for Test 2 for hydronic reheat than for electric reheat during the warm up period. This indicates that electric reheat may provide a more comfortable thermal environment than hydronic reheat during the warm-up and cool-down periods of each day.

4.3. Occupied PMV

For evaluation of PMV, M is set to 56.8 W/m^2 [10] to represent typical office activities and W is set to 0 W/m^2 assuming no external work is accomplished. The value of I_{cl} for Tests 1, 3, and 4 is set to 0.61 clo, which represents trousers and long-sleeve shirt for a typical summer day [10]. Due to cool weather conditions for Test 2, a higher value of I_{cl} of 0.96 clo is chosen to represent trousers and long-sleeve shirt plus suit jacket [10]. The room temperature data are used for T_a and T_{rad}. The VAV air flow is used for Q. The values of ϕ are measured by the comfort sensor located near the center of a room.

Values for PMV$_{om}$ are shown in Table 3. Recall that the uncertainty for PMV is around 10%. It is observed that all PMV$_{om}$ are negative ranging from −0.72 to −0.07. These PMV values imply that the rooms are slightly cool but still comfortable for the occupants. The PMV$_{om}$ values for economizer cooling are slightly higher than those for mechanical and mechanical and economizer cooling. For both the A- and B-Systems, PMV$_{om}$ values are about 40% higher for hydronic reheat than those for electric reheat for mechanical and mechanical and economizer cooling. For economizer cooling, PMV$_{om}$ values are about 42% higher for the A-System and about 36% higher for the B-System for

Table 3
Overall mean PMV[a]

Reheat	Mechanical and mechanical and economizer cooling			Economizer cooling
	Test 1	Test 3	Test 4	Test 2
E(A)	−0.70	−0.68	−0.52	−0.44
H(A)	−0.41	−0.39	−0.35	−0.32
E(B)	−0.72	−0.69	−0.73	−0.40
H(B)	−0.43	−0.47	−0.38	−0.33

[a]E and H, electric and hydronic reheats; A and B, A- and B-Systems.

hydronic reheat than those for electric reheat. These findings indicate that hydronic reheat provides a slightly warmer thermal environment than electric reheat during most of the time of a day.

4.4. Energy analysis

Consistent with Fig. 6, four electric and two hydronic energy uses for the HVAC system are calculated. For the analysis, HE consists of only HR because the heating coils were not operated during the tests and the heat loss along the heated water loop is taken to be negligible. To illustrate the values of these energy terms, results for daily energy usage for different days are displayed in Table 4 for Test 1, where the mechanical cooling mode is used. As noted previously, the uncertainties for an energy quantity are estimated to be less than 1%.

The observations for each energy term are reported in the same order as listed in Table 4 as follows:

1. Fan energy (FE): Supply and return fan energies are included in FE. For each system, the daily fan energies for electric and hydronic reheats are around 15 and 10 kW h and the fan power for electric reheat is 25–30% higher than that for hydronic reheat. This latter finding is attributed to the need to have a higher minimum air flow for electric reheat than for hydronic reheat.
2. Pump energy (PE): Pump energy for the cooling and heating coils as well as the water loop for hydronic reheat are included in PE and are typically around 4.8 and 4.4 kW h for electric and hydronic reheats.
3. Cooling coil energy (CC): For the A-System, CC for hydronic reheat is 40% lower than that for electric reheat. For the B-System, CC for hydronic reheat is 18% lower than that for electric reheat. In other words, the energy usage in the cooling coil for hydronic reheat is lower than that for electric reheat because of the lower air flow for hydronic reheat than that for electric reheat.
4. Electric reheat energy (ER): For test period 4.2, which corresponds to a day when both systems are operated using electric reheat, ER for the A- and B-Systems are similar. For the other test periods, ER for the B-System is nearly 50% higher than that for the A-System, where the difference may be attributed to different weather conditions for these test periods.
5. Total electric energy (EE): EE sums up the values for FE, PE, CC, and ER. For the considered test, CC accounts for a considerable portion of EE. EE for hydronic reheat is about 70% of that for electric reheat.
6. Total hydronic energy (HE): HE for this test is essentially zero implying that hydronic reheat is not used. For Test 3 (data not shown), which uses the economizer cooling mode for a cool day, HE ranges typically from 35 to 76 kW h. For a test period, when both systems use hydronic reheat, HEs for the A- and B-Systems are 39 and 34 kW h.

In summary, for a typical mechanical cooling day that uses electric reheat, FE, PE, CC, and ER are about 9, 2, 79, and 10% of TE (≅EE). For a typical mechanical cooling day that uses hydronic reheat, FE, PE, CC, and HR are about 8, 3, 87, and 2% of TE. This indicates that the AHU related energies are the major contributors to TE for mechanical cooling. For a typical economizer cooling day, FE and ER are about 15 and 85% of TE for electric reheat and FE, PE, and HR are about 16, 7, and 77% of TE for hydronic reheat. These results show that the VAV unit related energies are the major contributors to TE for the economizer cooling mode. The data indicated that, to compare the energy usage for electric and hydronic reheats, the weather conditions must be taken into consideration. This is undertaken in Section 4.5.

Table 4
Daily energies for test 1[a]

System	Re-heat	Test period	Electric energy					Hydronic energy (HE) (kW h)
			Fan (FE) (kW h)	Pump (PE) (kW h)	Cooling coil (CC) (kW h)	Electric reheat (ER) (kW h)	Total (EE) (kW h)	
A	H	1.2	10.8	4.4	116.0	0.0	131.3	0.3
A	H	2.2	9.7	4.4	97.6	0.0	111.6	0.3
A	H	2.3	9.4	4.1	95.8	0.0	109.3	0.3
A	H	2.4	10.8	4.1	110.8	0.0	126.0	0.3
A	E	3.2	15.2	3.8	159.4	6.7	185.5	0.0
A	E	3.3	14.6	3.8	149.1	12.9	180.5	0.0
A	E	3.4	14.6	3.8	146.8	17.9	183.1	0.0
A	E	4.2	14.6	3.8	136.5	16.4	171.4	0.0
B	H	1.2	11.7	5.0	128.9	0.0	145.3	0.9
B	E	2.2	15.2	4.1	151.8	24.0	195.1	0.0
B	E	2.3	15.2	4.1	151.2	25.2	196.0	0.0
B	E	2.4	15.5	4.1	152.1	14.4	185.8	0.0
B	H	3.2	12.6	5.0	139.2	0.0	156.8	0.9
B	H	3.3	11.1	5.0	121.9	0.0	138.0	0.6
B	H	3.4	10.8	4.7	115.1	0.0	131.0	0.6
B	E	4.2	15.2	4.1	141.8	17.6	178.7	0.0

[a] A and B: A- and B-Systems; E and H: electric and hydronic reheats.

4.5. Energy distribution

As previously noted and expected, the energy usage for either reheat mode depends partially on the weather conditions. An initial analysis using DD did not explain fully the behavior of the energies as a function of weather conditions. Hence, the energies were analyzed in terms of DD_s that accounts for solar energy. The daily values for CC, ER, and TE for electric reheat and CC, HR, and TE for hydronic reheat are plotted in Figs. 9 and 10 as a function of DD_s. The notation used to reference a result is A or B for either the A- or B-System followed by a numerical value that indicates the test number. Because CC is the major contributor of the energy usage for the AHU, only CC is displayed in Figs. 9a and 10a.

The values for DD_s are between −16.7 and 22.2 °C for the tests. Note that Test 2 has negative values for DD_s, Test 4 has both negative and positive values for DD_s, and Tests 1 and 3 have all positive values for DD_s. It is found that the corresponding control sequence for the AHU and VAV units gives a good indication of the energy distribution for the different weather conditions.

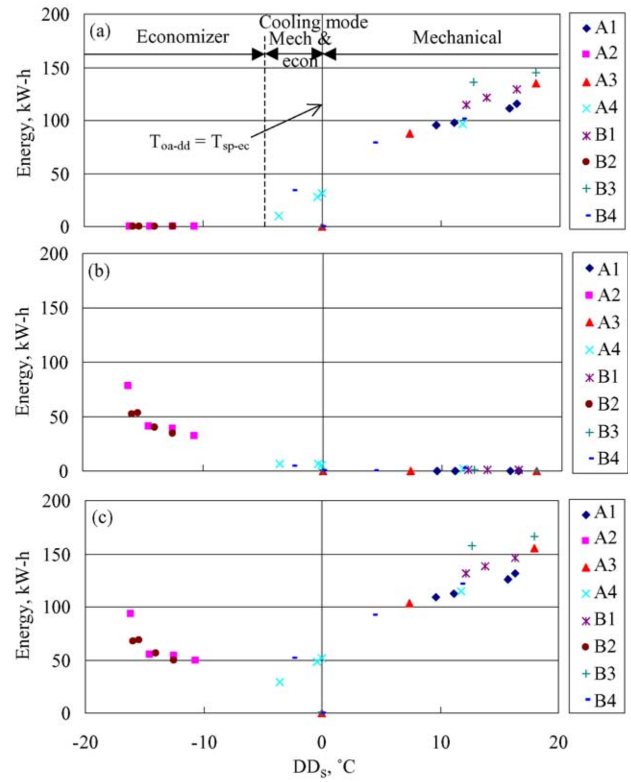

Fig. 10. Energies for hydronic reheat. (a) Cooling coil; (b) Hydronic reheat; (c) Total energy.

1. Cooling coil energy (CC): As previously mentioned, mechanical, mechanical and economizer, and economizer cooling modes are used for Tests 1 and 3, Test 4, and Test 2. As seen from the negative half planes in Figs. 9a and 10a, CC for Test 2 is zero due to the low outdoor air temperature and economizer cooling mode. Non-zero values for CC begin to appear when DD_s is greater than about −5.6 °C corresponding to the end of the economizer cooling mode and increase nearly linearly with DD_s through the mechanical and economizer cooling mode and into the mechanical cooling mode. From Fig. 9a (electric reheat), as DD_s increases, CC increases almost linearly until the values of DD_s reach about 11.1 °C and remains almost constant after that. As shown in Fig. 10a for hydronic reheat, CC continues to increase almost linearly with DD_s. The nearly constant values of CC at the higher values of DD_s are attributed to the condition that electric reheat has a higher minimum air flow across the reheat coil, therefore, causing the air flow across the cooling coil to be higher than that for hydronic reheat. This larger amount of air flow produces a larger cooling load for the cooling coil, which causes the cooing coil valve to be opened more for electric reheat than for hydronic reheat. At a wide-open position, the cooling coil valve is incapable of increasing the chilled water flow any more thereby causing CC to be nearly a constant value at the higher values of DD_s. When non-zero, at a given value of DD_s and excluding CC for $DD_s > 11.1$ °C, CC for electric reheat is about 60% higher than that for hydronic reheat.

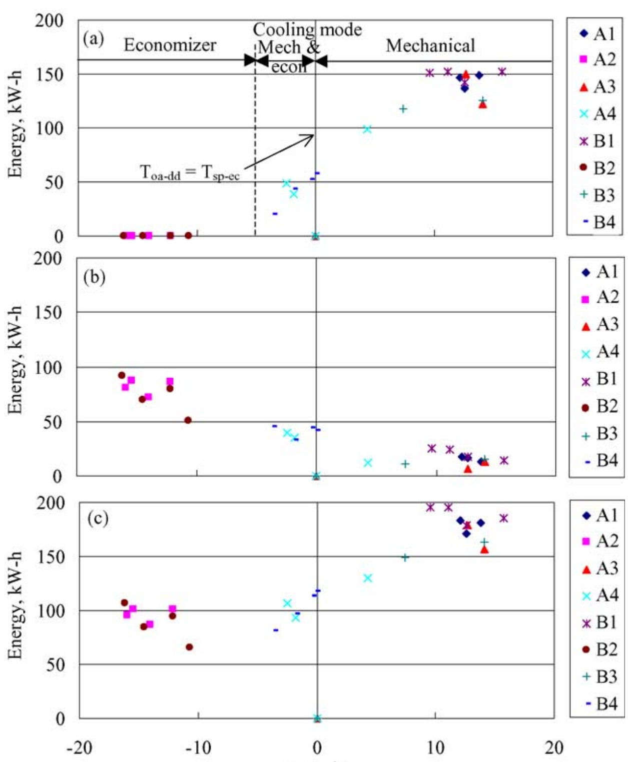

Fig. 9. Energies for electric reheat. (a) Cooling coil; (b) Electric reheat; (c) Total energy.

2. Reheat energy (ER or HR): The stages of electric reheat are modulated to maintain the room temperature near $T_{sp\text{–}ht}$ and the VAV damper is held at the minimum position. With the minimum air flow, ER decreases linearly

as DD_s increases as indicated by the data in Fig. 9b. ER decreases from 87.9 kW h when DD_s is around -16.7 °C to near 5.9 kW h when DD_s is around -16.7 °C.

The reduced supply of cooled air attributed to the lower minimum air flow results in lower heating requirements for hydronic reheat. Consequently, the VAV damper is not held at the minimum position all the time under hydronic reheat. The data in Fig. 10b illustrate that different groups of data behave differently according to the AHU cooling mode. For Tests 1 and 3 that have the lowest requirements of the reheat among the tests, HR is zero. For Tests 4 and 2, the VAV control sequence for hydronic reheat causes the HR to decrease not as linearly as for ER displayed in Fig. 9b. HR decreases from 58.6 kW h when DD_s is around -16.7 °C to near 5.9 kW h when DD_s is around -0 °C. Because of the higher minimum air flow for the AHU, ER is non-zero in the mechanical cooling mode where HR is zero. The VAV related energy is about 75 and 54% lower for hydronic reheat than that for electric reheat for mechanical and mechanical and economizer cooling modes. This implies that hydronic reheat is a relatively low energy reheat mode compared to electric reheat. The reason for this low energy characteristic for hydronic reheat is due to the lower requirement for the minimum air flow across the reheat coil.

3. Total energy (TE): The daily fan and pump energies are almost constant, varying from 14.7 to 16.1 kW h for electric reheat and from 8.8 to 14.7 kW h for hydronic reheat, so the TE values shown in Figs. 9c and 10c are basically the combinations of the energy distributions for the AHU and VAV unit. Values of TE for electric and hydronic reheats reach a minimum around $DD_s = -5.6$ °C, in other words, TE is the lowest at the boundary between the mechanical and economizer and economizer cooling modes. TE increases from this minimum point as DD_s increases due to the increasing CC, and increases as DD_s decreases due to the increasing reheat energy.

5. Conclusions

This study examines the energy consumption and thermal comfort of electric and hydronic reheats using experiments. Uncertainty analyses for the energy terms and PMV are introduced to define the accuracy of the results and to determine if the comparisons are meaningful. During the examination for the energy usages, weather effects are considered and the corresponding energy distributions are evaluated. The uncertainty analyses indicate that the uncertainties for each energy term are within 1% and that the uncertainty for the PMV is about 10%. The results show that the energy distributions are related to the weather conditions. The corresponding control sequences for the AHU and VAV units give a good indication of the energy usage for the different weather conditions. From the energy usage point of view, the comparisons between electric and hydronic reheats imply that the latter is a relatively low-energy reheat. Specifically, the AHU related energy for hydronic reheat is lower than that for electric reheat by about 24% when the AHU is operated in either the mechanical or mechanical and economizer cooling mode and 33% for the economizer cooling mode. The hydronic reheat energy for the VAV unit is lower than that for electric reheat by about 75% for either the mechanical or mechanical and economizer cooling mode and 54% for the economizer cooling mode. The major reason for the lower energy consumption of hydronic reheat is due to the lower requirement for the minimum air flow across the reheat coil. The comfort environments provided by electric reheat are slightly cooler than those provided by hydronic reheat.

Acknowledgements

This study was made possible through Grant No. 96-10a from the Iowa Energy Center.

References

[1] DOE, Annual Energy Outlook 1998. Department of Energy, Energy Information Administration, DOE/EIA-0383 (98), December 1997.
[2] D.C. Hittle, Controlling variable-volume systems, American Society of Heating, Refrigerating and Air Conditioning Engineers Journal (September 1997) 50–53.
[3] M.A. Reed, Conversion to VAV hood exhaust slashes fan horsepower, HPAC Journal (January 1994) 68–74.
[4] Y.S. Hung, H.N. Lam, Dynamic performance of an electronic zone air temperature control loop in a typical variable-air-volume air conditioning system, HVAC&R Research 5 (4) (1999) 317–337.
[5] M.M. Ardehali, T.F. Smith, Evaluation of HVAC system operational strategies for commercial buildings, Energy Conversion and Management 37 (9) (1996) 1469–1479.
[6] S. Winata, A study of energy usage in a variable air volume HVAC system, Master of Science thesis, Iowa State University, Ames, Iowa, 2001
[7] J.J. Hirsch & Associates, Public comments into the 2005 building energy efficiency standards, Building Performance Simulation Research and Consulting, Southern California Edison, Camarillo, California, 2001.
[8] G.D. Ander, VAV electric reheat, California Building Energy Efficiency Standards, Revisions for July 2003 Adoption, Camarillo, California, 2001.
[9] Energy Water Conservation Capital Projects, Campus Planning & Facilities Design, Rensselaer Polytechnic Institute, 2002. http://www.rpi.edu/dept/cpfd.
[10] ASHRAE Fundamentals Handbook, American Society of Heating, Refrigerating, and Air-Conditioning Engineers, Inc., Atlanta, Georgia, 1981.
[11] Iowa Energy Center, http://www.energy.iastate.edu/ers/, 2004.
[12] J.A. Duffie, W.A. Beckman, Solar engineering of thermal processes, Wiley, New York, 1980.
[13] H.W. Coleman, W.G. Steele, Experimentation and Uncertainty Analysis for Engineers, second ed., Wiley, New York, 1999.